Supplementary Information: Topological Engineering of High-Order Exceptional Points through Transformation Optics

Kaiyuan Wang Qi Jie Wang Matthew R. Foreman Yu Luo**

Kaiyuan Wang, Matthew R. Foreman
School of Electrical and Electronic Engineering, Nanyang Technological University, 50 Nanyang Avenue, Singapore 639798
Institute for Digital Molecular Analytics and Science, 59 Nanyang Drive, Singapore 636921
Email Address: matthew.foreman@ntu.edu.sg
Qi Jie Wang
School of Electrical and Electronic Engineering, Nanyang Technological University, 50 Nanyang Avenue, Singapore 639798
Centre for Disruptive Photonic Technologies, School of Physical and Mathematical Sciences, Nanyang Technological University, Singapore, Singapore
Yu Luo
National Key Laboratory of Microwave Photonics, Nanjing University of Aeronautics and Astronautics, Nanjing 211106, China
Email Address: yu.luo@nuaa.edu.cn

Keywords: *Non-Hermitian physics, exceptional points, transformation optics, nanoplasmonics*

1 Introduction

In our article we discuss the use of transformation optics for design of high order exceptional points in two-dimensional (2D) nanophotonic systems. Here we provide further mathematical details of our approach. In Section 2 we first derive the standard resonance condition for surface plasmon polariton (SPP) modes in a planar slab-like geometry. An alternative derivation is presented in Section 3 and extended to higher order geometries. Section 4.1 details how this result can be in turn used to identify second order exceptional points in an asymmetric core-shell nanowire structure. Sections 4.2 and 4.3 apply similar principles to study third and fourth order exceptional points in a coupled core-shell/monomer nanowire system and core-shell dimer system respectively.

2 Three layer resonance condition

We consider the geometry shown in Figure 1(a) comprising of three regions of relative electric permittivity ϵ_1, ϵ_2 and ϵ_3 respectively, separated by interfaces at $x = x_0$ and $x = x_0 + d$, and illuminated by a periodic array of electric line dipoles each with moment $\mathbf{\Delta}$. The line dipoles are assumed to lie in the left-most medium and located at $\mathbf{r}_m = (x_m, y_m) = (0, 2m\pi)$ for $m \in \mathbb{Z}$. Our choice of illumination is for later convenience when performing calculations in the transformed coordinate system, however, this choice does not affect the resonance condition.

We will assume that the quasi-static approximation holds, such that the electric potential $\phi(\mathbf{r})$ induced in the systems from the line dipoles satisfies Laplace's equation

$$\nabla^2\phi(\mathbf{r}) = -\frac{1}{2\pi\epsilon_0}\sum_{m=-\infty}^{m=+\infty}\frac{\mathbf{\Delta}\cdot(\mathbf{r}-\mathbf{r}_m)}{|\mathbf{r}-\mathbf{r}_m|^2} = \phi_0(\mathbf{r}), \tag{1}$$

where $\mathbf{r} = (x, y)$ is the 2D position vector and $\phi_0(\mathbf{r})$ is the source potential. The problem of determining the induced potential is easily solved in the Fourier domain [1, 2]. In an arbitrary plane x the source potential can be written in the form:

$$\phi_0(\mathbf{r}) = \frac{1}{2\pi}\int_{-\infty}^{\infty}\Phi_0(k, x)e^{iky}dk \tag{2}$$

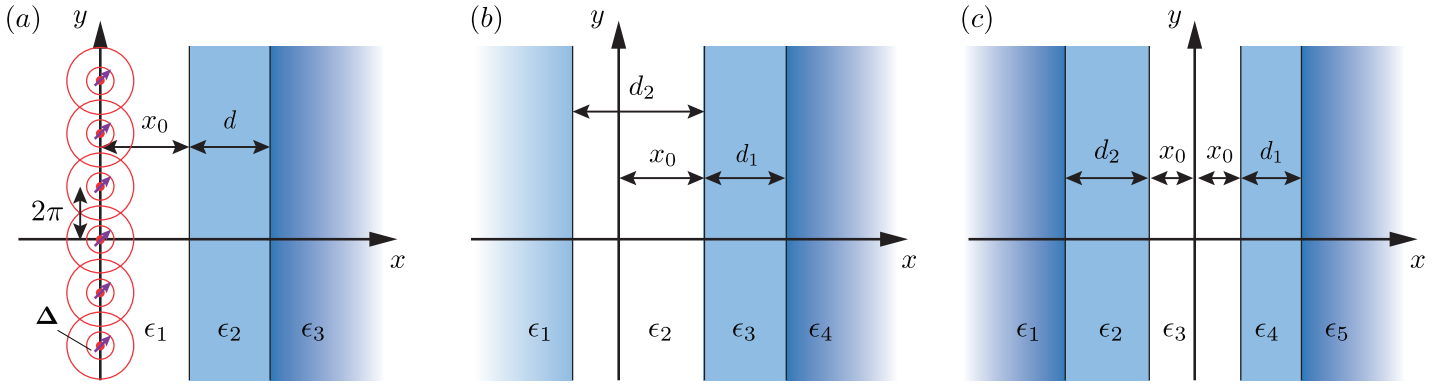

Figure 1: Schematics of 2D planar multilayer geometries considered comprising of (a) 3, (b) 4 and (c) 5 distinct material regions.

where

$$\Phi_0(k,x) = -\frac{1}{2\pi\epsilon_0}\sum_{m=-\infty}^{m=+\infty}\int_{-\infty}^{\infty}\frac{\boldsymbol{\Delta}\cdot(\mathbf{r}-\mathbf{r}_m)}{|\mathbf{r}-\mathbf{r}_m|^2}e^{-iky}dy \tag{3}$$

$$= -\frac{1}{2\pi\epsilon_0}\sum_{m=-\infty}^{m=+\infty}e^{-iky_m}\int\frac{\boldsymbol{\Delta}\cdot\mathbf{r}}{|\mathbf{r}|^2}e^{-iky}dy \tag{4}$$

$$= \begin{cases}\mathcal{A}_+(k)e^{-|k|x} & \text{if } x>0\\ \mathcal{A}_-(k)e^{|k|x} & \text{if } x<0\end{cases} \tag{5}$$

where

$$\mathcal{A}_\pm(k) = -\frac{1}{2\epsilon_0}\sum_{m=-\infty}^{m=+\infty}e^{-iky_m}(\pm\Delta_x + i\,\mathrm{sign}[k]\Delta_y) \tag{6}$$

$$= -\frac{1}{2\epsilon_0}\sum_{n=-\infty}^{n=+\infty}(\pm\Delta_x + i\mathrm{sign}[k]\Delta_y)\delta(k-n) \tag{7}$$

and $\delta[k]$ denotes the Dirac delta function. From Equations (5) and (7), we note that the Fourier spectrum of the source potential is a Dirac comb. Accordingly, only modes associated with integer spatial frequencies n can be excited by the chosen source distribution.

Each Fourier component of the source potential $\Phi_0(k)$ induces a potential across all space which can be expressed in the form

$$\Phi(k,x) = \begin{cases}\mathcal{B}(k)\,e^{iky+|k|x} & \text{for } x\le x_0\\ \mathcal{C}(k)\,e^{iky-|k|x}+\mathcal{D}(k)\,e^{iky+|k|x} & \text{for } x_0\le x\le x_0+d\\ \mathcal{E}(k)\,e^{iky-|k|x} & \text{for } x_0+d\le x\end{cases} \tag{8}$$

where as a consequence of the Dirac delta functions in Equation (7) $k=n$ ($n\in\mathbb{Z}$). Note the total potential in the Fourier domain is then $\Phi_0(k,x)+\Phi(k,x)$.

To find the resonance condition of the sheet geometry, we follow the standard procedure and enforce continuity of the tangential (normal) components of the electric (displacement) field $\mathbf{E}$ ($\mathbf{D}$). Noting then that $\mathbf{E}(\mathbf{r}) = -\nabla\phi(\mathbf{r})$ and $\mathbf{D}(\mathbf{r}) = \epsilon\mathbf{E}(\mathbf{r})$ respectively, for a single Fourier component we have at $x=x_0$ (assuming $x_0>0$)

$$\mathcal{A}_+(k)e^{-|k|x_0} + \mathcal{B}(k)e^{|k|x_0} = \mathcal{C}(k)e^{-|k|x_0} + \mathcal{D}(k)e^{|k|x_0} \tag{9}$$

$$\epsilon_1\left[\mathcal{A}_+(k)e^{-|k|x_0} - \mathcal{B}(k)e^{|k|x_0}\right] = \epsilon_2\left[\mathcal{C}(k)e^{-|k|x_0} - \mathcal{D}(k)e^{|k|x_0}\right]. \tag{10}$$

Similarly at $x = x_0 + d$ it follows that

$$\mathcal{C}(k)e^{-|k|(x_0+d)} + \mathcal{D}(k)e^{|k|(x_0+d)} = \mathcal{E}(k)e^{-|k|(x_0+d)} \tag{11}$$

$$\epsilon_2\left[\mathcal{C}(k)e^{-|k|(x_0+d)} - \mathcal{D}(k)e^{|k|(x_0+d)}\right] = \epsilon_3\mathcal{E}(k)e^{-|k|(x_0+d)}. \tag{12}$$

Solving Equations (9)–(12) for the unknown amplitudes $\mathcal{B}(k)$, $\mathcal{C}(k)$, $\mathcal{D}(k)$ and $\mathcal{E}(k)$, yields

$$\mathcal{B}(k) = \left[\frac{\epsilon_2-\epsilon_3}{\epsilon_2+\epsilon_3} + \frac{\epsilon_1-\epsilon_2}{\epsilon_1+\epsilon_2}e^{2|k|d}\right]\frac{e^{-2|k|x_0}}{e^{2|k|d}-e^{\beta}}\mathcal{A}_+(k) \tag{13}$$

$$\mathcal{C}(k) = \frac{2\epsilon_1}{\epsilon_1+\epsilon_2}\frac{e^{2|k|d}}{e^{2|k|d}-e^{\beta}}\mathcal{A}_+(k) \tag{14}$$

$$\mathcal{D}(k) = \frac{2\epsilon_1(\epsilon_2-\epsilon_3)}{(\epsilon_1+\epsilon_2)(\epsilon_2+\epsilon_3)}\frac{e^{-2|k|x_0}}{e^{2|k|d}-e^{\beta}}\mathcal{A}_+(k) \tag{15}$$

$$\mathcal{E}(k) = \frac{4\epsilon_1\epsilon_2}{(\epsilon_1+\epsilon_2)(\epsilon_2+\epsilon_3)}\frac{e^{2|k|d}}{e^{2|k|d}-e^{\beta}}\mathcal{A}_+(k) \tag{16}$$

where

$$e^{\beta} = \frac{(\epsilon_2-\epsilon_1)(\epsilon_2-\epsilon_3)}{(\epsilon_1+\epsilon_2)(\epsilon_2+\epsilon_3)}. \tag{17}$$

Finally, we note from Equations (13)–(16) that the induced potential scales with $[\exp(2|k|d) - \exp(\beta)]^{-1}$ regardless of source potential. Resonances in the system are thus seen to occur when

$$e^{2|k|d} = \frac{(\epsilon_2-\epsilon_1)(\epsilon_2-\epsilon_3)}{(\epsilon_1+\epsilon_2)(\epsilon_2+\epsilon_3)}. \tag{18}$$

3 Alternative derivation

In this section we again seek to determine the resonance condition, however, present an alternative derivation which enables us to calculate the corresponding mode potentials more easily. This approach furthermore enables easy extension to the higher order geometries shown in Figure 1(b) and (c). We begin by considering the second order case (Figure 1(a)), in which we seek bound surface modes whose potential distribution takes the form of Equation (8). We may express the tangential electric field components at $x = d_0$ and $x = d_0 + d$, denoted $E_{y,1}$ and $E_{y,2}$ respectively as

$$E_{y,1} = ik\,\mathcal{B}(k)e^{|k|x_0} \tag{19}$$

$$E_{y,1} = ik\left[\mathcal{C}(k)e^{-|k|x_0} + \mathcal{D}(k)e^{|k|x_0}\right] \tag{20}$$

$$E_{y,2} = ik\left[\mathcal{C}(k)e^{-|k|(x_0+d)} + \mathcal{D}(k)e^{|k|(x_0+d)}\right] \tag{21}$$

$$E_{y,2} = ik\,\mathcal{E}(k)e^{-|k|(x_0+d)}. \tag{22}$$

The normal components of the displacement, $D_{x,1}$ and $D_{x,2}$, can similarly be expressed

$$D_{x,1} = \epsilon_1|k|\,\mathcal{B}(k)e^{|k|x_0} \tag{23}$$

$$D_{x,1} = \epsilon_2|k|\left[-\mathcal{C}(k)e^{-|k|x_0} + \mathcal{D}(k)e^{|k|x_0}\right] \tag{24}$$

$$D_{x,2} = \epsilon_2|k|\left[-\mathcal{C}(k)e^{-|k|(x_0+d)} + \mathcal{D}(k)e^{|k|(x_0+d)}\right] \tag{25}$$

$$D_{x,2} = -\epsilon_3|k|\,\mathcal{E}(k)e^{-|k|(x_0+d)}. \tag{26}$$

Eliminating $\mathcal{B}(k)$, $\mathcal{C}(k)$, $\mathcal{D}(k)$, $\mathcal{E}(k)$, $D_{x,1}$ and $D_{x,2}$ from Equations (19)–(26) yields two linear equations for $E_{y,1}$ and $E_{y,2}$, which written in matrix form reads

$$\begin{bmatrix} 1+(\epsilon_2/\epsilon_1)\tanh(|k|d) & (\epsilon_3/\epsilon_1)\mathrm{sech}(|k|d) \\ -\mathrm{sech}(|k|d) & 1+(\epsilon_3/\epsilon_2)\tanh(|k|d) \end{bmatrix}\begin{bmatrix} E_{y,1} \\ E_{y,2} \end{bmatrix} \triangleq \mathbb{M}^{(2)}\mathbf{E}^{(2)} = \mathbf{0}_2 \tag{27}$$

where $\mathbf{0}_p$ is a $p \times 1$ vector of zeros. Equation (27) only has non-trivial solutions when the matrix $\mathbb{M}$ has zero determinant, i.e. $\det[\mathbb{M}^{(2)}] = 0$, or equivalently

$$(\epsilon_2^2 + \epsilon_1\epsilon_3)\tanh(|k|d) + \epsilon_2(\epsilon_1 + \epsilon_3) = 0. \tag{28}$$

It is easy to show that Equation (28) is equivalent to Equation (18). The advantage of expressing the resonance condition in the form of Equation (27) is that we can also determine the form of the potential and field distributions on resonance. Specifically, through Gaussian elimination it can be shown that the solution to Eq. (27) when Eq. (28) holds, is given by

$$\mathbf{E}^{(2)} = \begin{bmatrix} 1 \\ -\epsilon_3^{-1}[\epsilon_1\sinh(|k|d) + \epsilon_2\cosh(|k|d)] \end{bmatrix}. \tag{29}$$

Extension of the derivations given above to the three and four interface cases shown in Figure 1(b) and (c) follows analogous steps. We find for the three interface case that

$$\mathbb{M}^{(3)}\mathbf{E}^{(3)} = \begin{bmatrix} \mathcal{M}(d_2, \epsilon_2, \epsilon_1) & -\epsilon_2 & 0 \\ 0 & -\epsilon_3 & \mathcal{M}(d_1, \epsilon_3, \epsilon_4) \\ \mathcal{M}(d_2, \epsilon_1, \epsilon_2) & 0 & \mathcal{M}(d_1, \epsilon_4, \epsilon_3) \end{bmatrix} \begin{bmatrix} E_y(x_0 - d_2) \\ E_y(x_0) \\ E_y(x_0 + d_1) \end{bmatrix} = \mathbf{0}_3 \tag{30}$$

where, omitting the k dependence for clarity,

$$\mathcal{M}(d, \epsilon_a, \epsilon_b) \;\; = \;\; \epsilon_a\cosh(|k|d) + \epsilon_b\sinh(|k|d) \tag{31}$$

such that the resonance condition can be expressed as

$$\det[\mathbb{M}^{(3)}] = \epsilon_2\mathcal{M}(d_1, \epsilon_3, \epsilon_4)\mathcal{M}(d_2, \epsilon_1, \epsilon_2) + \epsilon_3\mathcal{M}d_1, \epsilon_4, \epsilon_3\mathcal{M}(d_2, \epsilon_2, \epsilon_2) = 0. \tag{32}$$

On resonance, the solutions to Equation (30) are of the form

$$\mathbf{E}^{(3)} = \begin{bmatrix} E_y(x_0 - d_2) \\ E_y(x_0) \\ E_y(x_0 + d_1) \end{bmatrix} = \begin{bmatrix} 1 \\ \epsilon_2^{-1}\mathcal{M}(d_2, \epsilon_2, \epsilon_1) \\ \epsilon_3\mathcal{M}(d_2, \epsilon_2, \epsilon_1)/[\epsilon_2\mathcal{M}(d_2, \epsilon_3, \epsilon_4)] \end{bmatrix}. \tag{33}$$

For the four interface geometry of Figure 1(c) we have $\mathbb{M}^{(4)}\mathbf{E}^{(4)} = \mathbf{0}_4$ where

$$\mathbb{M}^{(4)} = \begin{bmatrix} \mathcal{M}(d_2, \epsilon_2, \epsilon_1) & -\epsilon_2 & 0 & 0 \\ \coth(2|k|x_0)\mathcal{M}(d_2, \epsilon_1, \epsilon_2) & \epsilon_3 & 0 & \operatorname{cosech}(2|k|x_0)\mathcal{M}(d_1, \epsilon_5, \epsilon_4) \\ \operatorname{cosech}(2|k|x_0)\mathcal{M}(d_2, \epsilon_1, \epsilon_2) & 0 & \epsilon_3 & \coth(2|k|x_0)\mathcal{M}(d_1, \epsilon_5, \epsilon_4) \\ 0 & 0 & -\epsilon_4 & \mathcal{M}(d_1, \epsilon_4, \epsilon_5) \end{bmatrix} \tag{34}$$

with resonance condition

$$\begin{aligned} &\epsilon_3\mathcal{M}(d_1, \epsilon_4, \epsilon_5)\left[\epsilon_2\coth(2|k|x_0)\mathcal{M}(d_2, \epsilon_1, \epsilon_2) + \epsilon_3\mathcal{M}(d_2, \epsilon_2, \epsilon_1)\right] \\ &\quad + \epsilon_4\mathcal{M}(d_1, \epsilon_5, \epsilon_4)\left[\epsilon_2\mathcal{M}(d_2, \epsilon_1, \epsilon_2) + \epsilon_3\coth(2|k|x_0)\mathcal{M}(d_2, \epsilon_2, \epsilon_1)\right] = 0 \end{aligned} \tag{35}$$

and with corresponding solution, $\mathbf{E}^{(4)}$, of

$$\begin{bmatrix} E_y(-x_0 - d_2) \\ E_y(-x_0) \\ E_y(x_0) \\ E_y(x_0 + d_1) \end{bmatrix} = \begin{bmatrix} 1 \\ \epsilon_2^{-1}\mathcal{M}(d_2, \epsilon_2, \epsilon_1) \\ \epsilon_2^{-1}\cosh(2|k|x_0)\mathcal{M}(d_2, \epsilon_2, \epsilon_1) + \epsilon_3^{-1}\sinh(2|k|x_0)\mathcal{M}(d_2, \epsilon_1, \epsilon_2) \\ -[\epsilon_2\cosh(2|k|x_0)\mathcal{M}(d_2, \epsilon_1, \epsilon_2) + \epsilon_3\sinh(2|k|x_0)\mathcal{M}(d_2, \epsilon_2, \epsilon_1)]/[\epsilon_2\mathcal{M}(d_1, \epsilon_5, \epsilon_4)] \end{bmatrix}. \tag{36}$$

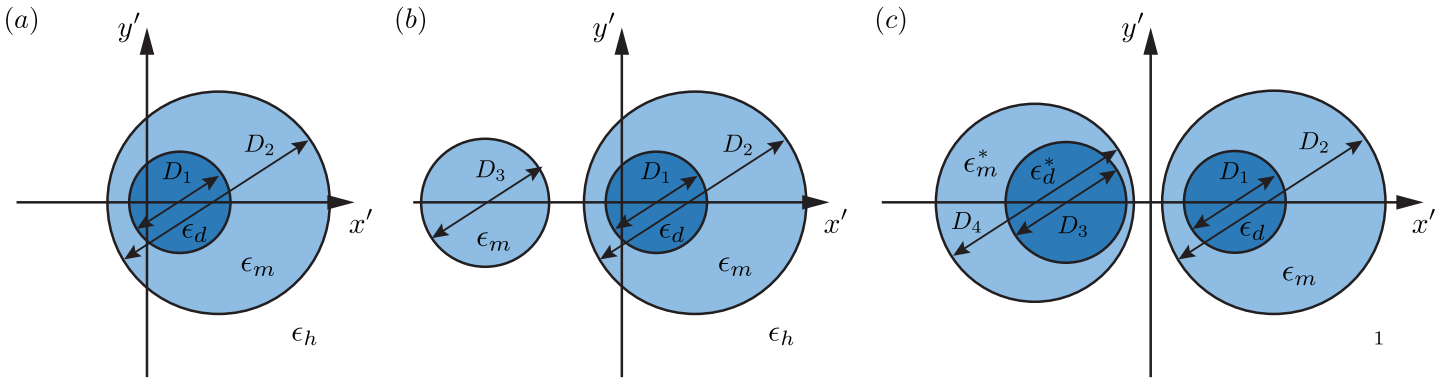

Figure 2: Schematics of geometries from Figure 2 under the action of the conformal transform given by Eq. (37), with material choices considered in Sections 4.1-4.3

4 Engineering exceptional points in nanowire systems

To study the properties of nanowire systems we can apply the principles of transformation optics to transform from the planar geometries of Figure 1, to those shown in Figure 2. Specifically, defining $w = x + iy$ in the original coordinates, and $w' = x' + iy'$ in the transformed coordinates we use the conformal transform

$$w' = \frac{g}{\exp(w) - 1} \tag{37}$$

where g is a constant that controls the size of the transformed cylinder(s). Specifically, the diameters of the cylinders for the core-shell nanowire of Figure 2(a) are

$$D_1 = \frac{g}{\exp(x_0 + d) - 1} + \frac{g}{\exp(x_0 + d) + 1} = g\,\mathrm{cosech}(x_0 + d) \tag{38}$$

$$D_2 = \frac{g}{\exp(x_0) - 1} + \frac{g}{\exp(x_0) + 1} = g\,\mathrm{cosech}(x_0) \tag{39}$$

For the core-shell and monomer structure shown in Figure 2(b) we have $D_1 = g\,\mathrm{cosech}(x_0 + d_2)$, $D_2 = g\,\mathrm{cosech}(x_0)$ and $D_3 = g\,\mathrm{cosech}(x_0 - d_2)$, whilst for the core-shell dimer geometry of Figure 2(c) we have similarly $D_1 = g\,\mathrm{cosech}(x_0 + d_1)$, $D_2 = D_4 = g\,\mathrm{cosech}(x_0)$ and $D_3 = g\,\mathrm{cosech}(x_0 + d_2)$.

Under the conformal transform the electrostatic potential is preserved [3], i.e. $\phi(x, y) = \phi'(x', y')$ whilst the electric permittivity and magnetic permeability tensors transform according to $\overline{\overline{\epsilon}}'_j = \epsilon_j \mathbb{J}\mathbb{J}^T/\det[\mathbb{J}]$ and $\overline{\overline{\mu}}'_j = \mu \mathbb{J}\mathbb{J}^T/\det[\mathbb{J}]$, where we have assumed all media are isotropic in the origin system, and

$$\mathbb{J} = \frac{g}{2(\cosh x \cos y)^2} \begin{bmatrix} 1 - \cosh x \cos y & -\sinh x \sin y & 0 \\ \sinh x \sin y & 1 - \cosh x \cos y & 0 \\ 0 & 0 & 2g^{-1}(\cosh x - \cos y)^2 \end{bmatrix} \tag{40}$$

is the Jacobian matrix for the transform given in Equation (37). Consequently the transformed tensors are of the form

$$\frac{\overline{\overline{\epsilon}}'_j}{\epsilon_j} = \frac{\overline{\overline{\mu}}'_j}{\mu_j} = \begin{bmatrix} 1 & 0 & \\ 0 & 1 & 0 \\ 0 & 0 & 4(\cos y - \cosh x)^2/g^2 \end{bmatrix}. \tag{41}$$

In the quasi-static limit, in which the dimensions of the relevant regions of interest are smaller than the optical wavelength, we may neglect the retardation effects as described by the spatial dependence of these material tensors. Consequently, we see that the electric permittivity and magnetic permeability of each region are also preserved under the action of Equation (37). Furthermore, we note that solution of the electrostatic problem (as described by Laplace's equation) restricts our discussion to transverse-magnetic (TM, or equivalently p-polarised) modes [4].

4.1 Core-shell nanowire (2nd order EP)

With the transformation complete, we now consider the asymmetric core-shell geometry shown in Figure 2(a). We consider a metallo-dielectric core-shell nanowire in a host material, such that $\epsilon_1 = \epsilon_h$, $\epsilon_2 = \epsilon_m$ and $\epsilon_3 = \epsilon_d$ whereby the resonance condition becomes

$$(\epsilon_m^2 + \epsilon_h\epsilon_d)\tanh(nd) + \epsilon_m(\epsilon_d + \epsilon_h) = 0. \tag{42}$$

Note that the periodicity in the transform implies $k = n$ ($n \in \mathbb{Z}$) in a similar fashion to that seen in Section 2 and that ϵ_d is in general complex accounting for gain or loss in the dielectric. Note also that generally, solutions to Equation (2) require $n \neq 0$. Expressing Equation (42) as a quadratic equation in ϵ_m, i.e.,

$$\epsilon_m^2 \tanh(nd) + \epsilon_m(\epsilon_d + \epsilon_h) + \epsilon_h\epsilon_d \tanh nd = 0 \tag{43}$$

we can solve for values ϵ_m, or equivalently (by virtue of the material dispersion) optical frequencies, at which resonances occur. The resonant modes however become degenerate when Equation (43) has a repeated root, i.e. when

$$(\epsilon_h + \epsilon_d)^2 = 4\epsilon_h\epsilon_d \tanh^2(nd). \tag{44}$$

or equivalently

$$\epsilon_d = \epsilon_h[2\tanh^2(nd) - 1 \pm 2i\tanh(nd)\mathrm{sech}(nd)]. \tag{45}$$

Substituting Equation (44) into Equation (43) and solving subsequently yields

$$\epsilon_m = -\frac{\epsilon_h + \epsilon_d}{2}\coth nd = -\epsilon_h[\tanh(nd) \mp i\mathrm{sech}(nd)]. \tag{46}$$

4.2 Coupled core-shell/monomer nanowires (3rd order EP)

We now consider the coupled nanowire structures depicted in Figure 2(b) where we assume $\epsilon_1 = \epsilon_m$, $\epsilon_2 = 1$, $\epsilon_3 = \epsilon_m$ and $\epsilon_4 = \epsilon_d$. Note that the two wire system depicted requires $d_2 > x_0$, otherwise a single three-layer nanowire structure results which is not our case of interest. With these replacements Equation (32) can be written as a cubic equation in ϵ_m

$$A\epsilon_m^3 + B\epsilon_m^2 + C\epsilon_m + D = 0 \tag{47}$$

where

$$\begin{aligned}
A &= \sinh(nd_1)\sinh(nd_2) && (48)\\
B &= \epsilon_h\cosh(nd_1)\cosh(nd_2) + \epsilon_h\sinh(nd_1)\cosh(nd_2) + \epsilon_d\cosh(nd_1)\sinh(nd_2) && (49)\\
C &= \epsilon_h\epsilon_d\cosh(nd_1)\cosh(nd_2) + \epsilon_h\epsilon_d\sinh(nd_1)\cosh(nd_2) + \epsilon_h^2\cosh(nd_1)\sinh(nd_2) && (50)\\
D &= \epsilon_d\epsilon_h^2\sinh(nd_1)\sinh(nd_2) && (51)
\end{aligned}$$

and $n \neq 0$. The roots of Equation (47) are all identical if

$$3AC - B^2 = 0 \tag{52}$$

$$27A^2D - 9ABC + 2B^3 = 0 \tag{53}$$

and take the form

$$\epsilon_m = -\frac{B}{3A} = \frac{1}{3}\left[\epsilon_h[1 + \coth(nd_1)]\coth(nd_2) + \epsilon_d\coth(nd_1)\right] \tag{54}$$

as discussed in the main text.

4.3 Coupled core-shell/core-shell nanowires (4th order EP)

Finally, we consider the core-shell dimer type structure shown in Figure 2(c). We assume a parity time symmetric configuration whereby $d_1 = d_2 = d$, $\epsilon_1 = \epsilon_d^*$, $\epsilon_2 = \epsilon_m^*$, $\epsilon_3 = 1$, $\epsilon_4 = \epsilon_m$ and $\epsilon_5 = \epsilon_d$. We further assume $\epsilon_m = \epsilon_\infty - \omega_p^2/\omega^2 + i\alpha$, whereas $\epsilon_d = \epsilon - i\beta$. Substituting these parameters into Equation (35) yields the polynomial express

$$A\omega^8 + B\omega^6 + C\omega^4 + D\omega^2 + E = 0 \tag{55}$$

where

$$\begin{aligned} A = \frac{1}{8}\text{cosech}\,(nx_0)\,\text{sech}\,(nx_0)\Big[& \left(\alpha^2 + (\epsilon_\infty - 1)^{\,2}\right)\left(\alpha^2 + \beta^2 + \epsilon^2 + \epsilon_\infty^2\right)\sinh\left[2n\,(x_0 - d)\right] \\ & + 2\left(\alpha^2 + (\epsilon_\infty - 1)^{\,2}\right)(\alpha\beta - \epsilon\epsilon_\infty)\cosh\left[2n\,(x_0 - d)\right] \\ & - 2\left(\alpha^2 + \epsilon_\infty^2 - 1\right)\left(\alpha^2 - \beta^2 - \epsilon^2 + \epsilon_\infty^2\right)\sinh\left[2nx_0\right] \\ & + 8\alpha\,(\alpha\epsilon + \beta\epsilon_\infty)\cosh\left[2nx_0\right] \\ & + \left(\alpha^2 + (\epsilon_\infty + 1)^{\,2}\right)\left(\alpha^2 + \beta^2 + \epsilon^2 + \epsilon_\infty^2\right)\sinh\left[2n\,(x_0 + d)\right] \\ & + 2\left(\alpha^2 + (\epsilon_\infty + 1)^{\,2}\right)(\alpha\beta - \epsilon\epsilon_\infty)\cosh\left[2n\,(x_0 + d)\right]\Big] \end{aligned} \tag{56}$$

$$\begin{aligned} B = \frac{1}{4}\omega_p^2\text{cosech}\,(nx_0)\,\text{sech}\,(nx_0)\Big[& \left(\alpha^2\,(1 - 2\epsilon_\infty) - (\epsilon_\infty - 1)\left(\beta^2 + \epsilon^2 + \epsilon_\infty\,(2\epsilon_\infty - 1)\right)\right)\sinh\left[2n\,(x_0 - d)\right] \\ & + \left(\alpha^2\epsilon - 2\alpha\beta\,(\epsilon_\infty - 1) + \epsilon\epsilon_\infty\,(3\epsilon_\infty - 4) + \epsilon\right)\cosh\left[2n\,(x_0 - d)\right] \\ & + 2\epsilon_\infty\left(2\alpha^2 - \beta^2 - \epsilon^2 + 2\epsilon_\infty^2 - 1\right)\sinh\left[2nx_0\right] - 4\alpha\beta\cosh\left[2nx_0\right] \\ & + \left(-\alpha^2\,(2\epsilon_\infty + 1) - (\epsilon_\infty + 1)\left(\beta^2 + \epsilon^2 + 2\epsilon_\infty^2 + \epsilon_\infty\right)\right)\sinh\left[2n\,(x_0 + d)\right] \\ & + \left(\alpha^2\epsilon - 2\alpha\beta\,(\epsilon_\infty + 1) + \epsilon\,(\epsilon_\infty + 1)\,(3\epsilon_\infty + 1)\right)\cosh\left[2n\,(x_0 + d)\right]\Big] \end{aligned} \tag{57}$$

$$\begin{aligned} C = \frac{1}{4}\omega_p^4\text{cosech}\,(2nx_0)\Big[& \left(1 + 2\alpha^2 + \beta^2 + \epsilon^2 - 6\epsilon_\infty\,(\epsilon_\infty - 1)\right)\sinh\left[2n\,(x_0 - d)\right] \\ & + \left(\epsilon\,(4 - 6\epsilon_\infty) + 2\alpha\beta\right)\cosh\left[2n\,(x_0 - d)\right] \\ & + \left(1 + 2\alpha^2 + \beta^2 + \epsilon^2 + 6\epsilon_\infty\,(\epsilon_\infty + 1)\right)\sinh\left[2n\,(x_0 + d)\right] \\ & + \left(-2\alpha\beta + 6\epsilon\epsilon_\infty + 4\epsilon\right)\cosh\left[2n\,(x_0 + d)\right] \\ & + \left(1 - 2\alpha^2 + \beta^2 + \epsilon^2 - 6\epsilon_\infty^2\right)2\sinh\left[2nx_0\right]\Big] \end{aligned} \tag{58}$$

$$D = -\omega_p^6\Big[4\epsilon_\infty\sinh[nd]\coth\left[nx_0\right] + \cosh[nd]\left(2\epsilon\coth\left[nx_0\right] + \coth^2\left[nx_0\right] + 1\right)\Big]\sinh[nd]\tanh\left[nx_0\right] \tag{59}$$

$$E = \omega_p^8\sinh^2(nd) \tag{60}$$

Equation (55) is a quartic equation in ω^2, the solutions to which are identical if

$$8AC - 3B^2 = 0 \tag{61}$$

$$B^3 - 4ABC + 8A^2D = 16AB^2C - 64A^2BD - 3B^4 + 256A^3E = 0 \tag{62}$$

Denoting these solutions as $\Xi = \omega_r^2 = -B/4A$, we can then find the eigenfrequencies $\omega_r = \pm\sqrt{\Xi}$, where solutions for which the real part is negative are discarded.

References

[1] D. Y. Lei, A. Aubry, S. A. Maier, and J. B. Pendry, "Broadband nano-focusing of light using kissing nanowires," New J. Phys. 12, 093030 (2010).

[2] A. Aubry, D. Y. Lei, S. A. Maier, and J. B. Pendry, "Plasmonic Hybridization between Nanowires and a Metallic Surface: A Transformation Optics Approach," ACS Nano 5, 3293–3308 (2011).

[3] J. Zhang, J. B. Pendry, and Y. Luo, "Transformation optics from macroscopic to nanoscale regimes: a review," Adv. Photon. 1, 014001 (2019).

[4] J. B. Pendry, "Negative Refraction Makes a Perfect Lens," Phys. Rev. Lett. 85, 3966–3969 (2000).